

# K&C Science Report – Phase 2

## Regional Mapping of Forest Growth Stage, Queensland, Australia, through Integration of ALOS PALSAR and Landsat Foliage Projective Cover.

Richard M. Lucas, John Armston<sup>2</sup>, Joao Carreiras<sup>3</sup>, Arnon Accad<sup>4</sup>

Dan Clewley and Peter Bunting

*Institute of Geography and Earth Sciences, Aberystwyth University, Aberystwyth, Ceredigion, United Kingdom, SY23 2EJ*

<sup>2</sup>*Queensland Department of Natural Resources and Water (QDNRW),  
Climate Building, 80 Meiers Road, Indooroopilly, Queensland, 4068.*

<sup>3</sup>*Instituto de Investigação Científica Tropical (ICT), Departamento de Ciências Naturais,  
Unidade Desenvolvimento Global, Rua João de Barros, 27, 1300-319 Lisboa, Portugal.*

<sup>4</sup>*Queensland Herbarium, Environmental Protection Agency, Brisbane Botanic Gardens,  
Mt. Coot-tha Road, Toowong, Brisbane, Queensland, 4066, Australia.*

**Abstract**—ALOS PALSAR 50 m spatial resolution strip data acquired over northern/eastern Australia during 2007, 2008 and 2009 were combined to generate mosaics for Queensland and New South Wales. For each year, strips acquired during relatively dry conditions, determined through reference to daily Advanced Microwave Scanning Radiometer-EOS (AMSR-E) effective vegetation water ( $\text{kg m}^{-2}$ ) and soil moisture ( $\text{g cm}^{-3}$ ) surfaces, provided the most seamless mosaics when combined. To support regional mapping of above ground biomass (AGB), the same suite of allometric equations were applied to plot-based measures of tree size obtained from over 2700 plots (1139 locations) distributed across a diversity of vegetation structural formations. Regardless of moisture conditions, L-band HV topographically normalized backscattering intensities backscatter ( $\sigma_r$ ) increased asymptotically with AGB, with the apparent saturation level being greatest for forests and least for open woodlands. Whilst a single algorithm was used to generate maps of AGB for Queensland and also NSW, several relationships between L-band HV  $\sigma_r$  and AGB could be defined as a function of forest structural type and/or growth stage suggesting potential for further refinement of retrieval algorithms. Whilst the algorithms for retrieval can be applied to map AGB in 2007, 2008 and 2009, residual moisture effects compromise the detection of changes in woody vegetation. For the Brigalow Belt Bioregion of SE Queensland, the combination of ALOS PALSAR L-band HH and HV and Landsat Foliage Projected Cover (FPC) allowed differentiation and mapping of remnant from non-remnant vegetation (> 90 % correct) and two growth stages (early and late regrowth). Non-linear estimation techniques were also evaluated for their potential to retrieve structural attributes (height and density) from L-band SAR data. The study has demonstrated the use of ALOS PALSAR data, either singularly or in combination with Landsat sensor data, for regional mapping of AGB and growth stage in Australia and also identified where further research can be directed to increase the robustness of retrieved biophysical attributes and accuracies in growth stage classifications.

**Index Terms**—ALOS PALSAR, K&C Initiative, Forest Theme, forest growth stage, Queensland, Australia.

## I. INTRODUCTION

### A. Approaches to discriminating and mapping growth stage

Discriminating and mapping different growth stages of woody vegetation (primarily shrublands, woodlands and forests) is important for quantifying current stocks of biomass (carbon) contained and the extent to which regenerating vegetation is recovering carbon lost previously through clearing or degradation. Knowledge of vegetation growth stage can also inform on the distribution, type and abundance of flora and fauna across landscapes and hence biodiversity (e.g., [1, 2]). An understanding of how past land use and types as well as natural processes (e.g., succession) and events (fire, drought) impact on the ability of woody vegetation to regenerate following previous loss or disturbance is also important for developing options for sustainable land management and ensuring long term maintenance of ecosystem value and services.

The Japan Aerospace Exploration Agency (JAXA) Kyoto and Carbon (K&C) Initiative aimed to evaluate and demonstrate the potential of Advanced Land Observing Satellite (ALOS) Phased Array L-band SAR (PALSAR) data for regional applications relating to carbon cycle science, conservation of biodiversity and international conventions [3]. In Phase 1 of the K&C, our research focused on exploring approaches to discriminating and mapping forest growth stages across Queensland, Australia. Of these, the establishment of empirical relationships between L-band HH and/or HV data and above ground biomass (AGB) was considered, as AGB is typically regarded as a surrogate for growth stage. A second approach was to integrate ALOS PALSAR and Landsat-derived Foliage Projected Cover (FPC) to differentiate several discrete stages of growth. These methods were applied to prototype areas and preliminary products generated. A limitation of applying these methods for map generation across northern Australia, however, was that large differences in brightness were observed between

image strips and over time, with this attributed to the large variation in ground moisture [4].

### B. Phase 2 project objectives

In Phase 2, the objective was to further develop and apply approaches to quantifying vegetation growth stages at a regional level, focusing primarily on the State of Queensland and regenerating forests in particular. A key component was to understand and overcome the limitations associated with surface moisture effects. The application of these approaches in other regions (New South Wales and the Northern Territory) was also evaluated. A third approach to growth stage classification was also investigated, with this focusing on the use of a non-linear estimation algorithm for retrieving structural attributes (e.g., height and density) from ALOS PALSAR data with inclusion of Landsat Foliage Projected Cover (FPC). The study further sought to establish whether changes in the woody structure of vegetation could be reliably detected using time-series of L-band SAR data.

## II. STUDY AREA

The study focused primarily on the state of Queensland, where a diversity of vegetation occurs, ranging from tropical rainforest to low open mallee. Across the state, extensive areas of vegetation are regarded as remnant (i.e., the dominant canopy is > 70% of the height and > 50% of the cover relative to the undisturbed height and cover of that stratum and is dominated by species characteristic of the vegetation's undisturbed canopy [5]). Nevertheless, many areas classified as remnant have suffered disturbance from natural processes (e.g., drought) or events (e.g., fire) and are at varying stages of succession.

Large area clearing of native vegetation followed European settlement in the late 1700s. The clearing of vegetation has historically been most significant in the south central and south-eastern regions, and has been particularly extensive since the 1950s. Of the 13 bioregions in Queensland, the Brigalow Belt Bioregion, has experienced amongst the highest rates of clearance, with less than 10% of regional ecosystems (REs) with brigalow (*Acacia harpophylla*) as a component remaining. However, within this bioregion, extensive regeneration is occurring, with most being relatively even-aged because of clearing (often through chaining and bulldozing; [6]) and abandonment over a similar time frame and across large areas. Patchy and more discontinuous areas of regrowth also occur where clearing methods such as ring-barking and stem injection have been employed. These diverse methods of clearing lead to differences in the capacity of regrowing vegetation to recover both carbon and biodiversity to pre-disturbance levels.

## III. AVAILABLE DATA

### A. Satellite sensor data.

For Queensland, ALOS PALSAR fine beam dual (FBD) strip data were provided by the JAXA Kyoto and Carbon (K&C) Initiative for 2007, 2008 and 2009 (Figure 1). Strip data were also provided for the Northern Territory and New

South Wales. All data were provided at 50 m spatial resolution, in slant-range geometry, amplitude format, and 64 looks (4 in range and 16 in azimuth), with a swath width approximating 70 km. Following a request to JAXA, all strip data acquired over the region were provided, giving a maximum of three dates per strip for each year. Fine beam dual (FBD) data were also provided and used to develop approaches to retrieval of AGB and structural attributes and classification of growth stages.

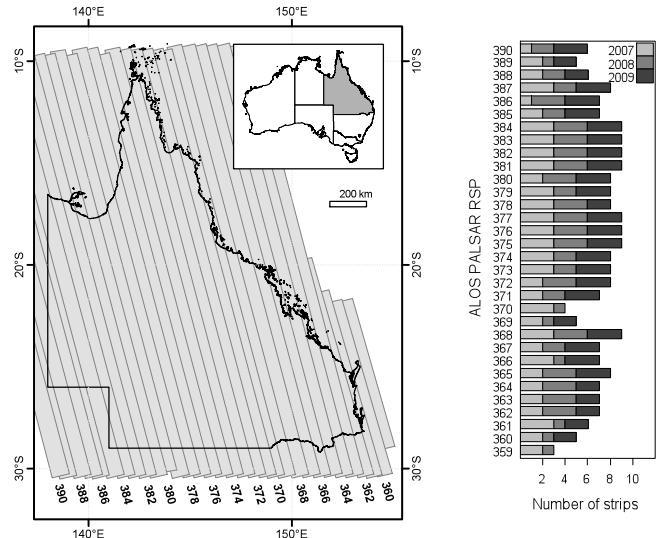


Figure 1. ALOS PALSAR K&C strip data (2007–2009) provided by JAXA.

## IV. DATA PREPROCESSING

### A. Pre-processing of strip data

The ALOS PALSAR data were converted to intensity and calibrated (absolute calibration) using Gamma SAR processing software [7, 8]. Geocoding of the strip data was undertaken with the Gamma Differential Interferometry and Geocoding (DIFF and GEO) suite and assisted using Landsat Enhanced Thematic Mapper (ETM+) panchromatic mosaics for all UTM zones (54 to 56 for Queensland, 52-53 for the Northern Territory). The median RMSE in both range and azimuth, defined with respect to the polynomial model fit, was less than 0.25 pixels (12.5 m), with this being consistent between years (Figure 2).

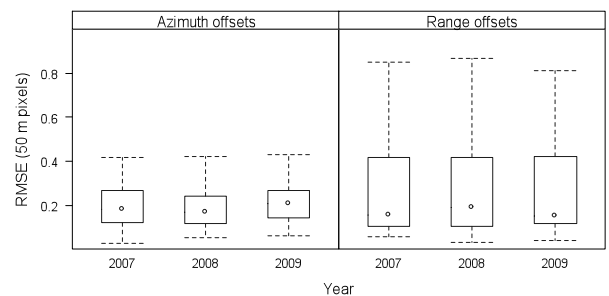


Figure 2. Distribution of strip registration RMSE in range and azimuth directions for each year of data acquisition.

Errors were generally greater in range than azimuth and outliers were associated primarily with those strips containing a significant amount of ocean as the number and distribution of matching features within the SAR and Landsat data extents were insufficient.

A particular benefit of geocoding using the Landsat sensor data was that all outputs were then registered to and could be integrated with existing statewide datasets. These included:

- a) Annual land cover change datasets based primarily on Landsat Foliage Projected Cover (FPC) data generated by QDERM for each year from 1988 [9, 10].
- b) Regional Ecosystem (RE) mapping generated by the Queensland Herbarium of the Queensland Department of Environment and Resource Management (QDERM) [11] and undertaken at a scale of 1:100,000 (Some coastal areas, including parts of Southeast Queensland and the Wet Tropics bioregions, were mapped at a larger (1:50,000) scale)

The combination of the land cover change and RE datasets has allowed losses of vegetation by forest type to be spatially quantified for Queensland as part of an existing statewide program of vegetation change monitoring and areas regarded as remnant or non-remnant to be defined.

Following geocoding, simple corrections for local ground scattering area and local incidence angle were undertaken, with the resulting strip data being analysed in units of topographically normalized backscattering intensities,  $\sigma_f^0$ . The corrections were based on the theory outlined in [12] and the same as those undertaken in other K&C research [13,14].

### B. Compositing and mosaicing.

For each year and Reference System for Planning (RSP), the acquisition date with the minimum average HH  $\sigma_f^0$  was selected for mosaicing. The HH polarisation was used because of greater sensitivity to variations in ground (soil and effective vegetation) water content [4]. Near range pixels were selected over far range pixels to preserve original  $\sigma_f^0$  values in the final mosaics. Problems with image quality at near and far range due to antenna pattern reduction were avoided by masking the power range loss. Spatial metadata are also created to accompany the final mosaics including the acquisition date (number of days since launch), and layover/shadow/water masks.

To provide independent indicators of surface moisture conditions for each RSP, Aqua Advanced Microwave Scanning Radiometer-EOS (AMSR-E; launched May 2002) daily effective vegetation water content and soil moisture estimates were sourced through the National Snow and Ice Data Center (NSIDC; [15, 16], updated daily). The soil moisture estimates are near surface (in the top ~1 cm) and are in units of  $g\ cm^{-3}$ . The effective vegetation water content, which includes the effects of large scale surface roughness, represents the amount of water ( $kg\ m^{-2}$ ) in the vertical column of vegetation. In both cases, the estimates are averaged over the retrieval footprint.

Ascending Aqua passes were used because comparison of the AMSR-E surfaces with SILO daily rainfall surfaces suggested greater sensitivity than descending passes to rainfall

events and the subsequent retention of moisture. Comparisons with rainfall surfaces are provided in [4]. The use of ascending passes is also consistent with other soil moisture research in Australian savanna environments [17]. To balance reducing noise in the data with preserving short-term variability and ensure complete ‘daily’ spatial coverage for Queensland, a 5-day boxcar average filter was applied to the AMSR-E time-series prior to extraction.

Example time series of SILO daily rainfall [18] and AMSR-E soil and vegetation water content for 2007 are shown in Figure 3, together with the timing of PALSAR FBD overpasses. Key points of note are:

- a) Whilst FBD data are typically acquired during the dry season, they still often intersect rainfall events.
- b) The general correspondence between the peaks of rainfall and effective vegetation moisture content and to a lesser extent soil moisture.
- c) The low temporal variation in soil moisture over time, especially over the mixed species forest site.

Where vegetation occurs, even if the cover is moderate, soil moisture estimates are known to be less reliable or inaccurate [19]. Estimates of effective vegetation water content include the combined effect of vegetation and large-scale surface roughness, but temporal changes can be interpreted primarily as changes in vegetation water content since surface roughness is relatively constant over time at the spatial resolution of the product [20].

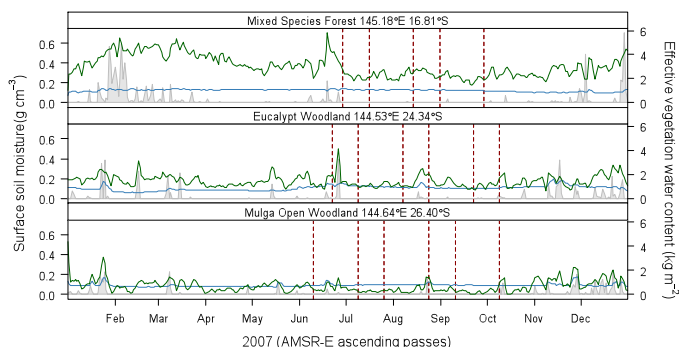


Figure 3. The range of environmental conditions in 2007 for three sites with contrasting vegetation cover compared to the timing of ALOS PALSAR overpasses (dashed vertical lines). The AMSR-E surface soil moisture (blue line) and effective vegetation water content (green line) are shown. The timing and relative magnitude of rainfall events (SILO daily rainfall; filled grey) is also shown.

### C. Statewide mosaics 2007-2009 and impacts of ground moisture

The statewide mosaics produced for Queensland for 2007, 2008 and 2009 (based on minimum average HH  $\sigma_f^0$ ) are shown in Figure 4, along with coincident date mosaics of AMSR-E soil moisture and effective vegetation water content. Areas of water, layover and shadow have been masked. In the 2008, and

to a lesser extent, the 2007 mosaic, differences in brightness within and between strips is evident, with this being most noticeable in the region centred on Carnarvon Gorge in central Queensland.

The residual banding in the 2007 and 2008 mosaics shows a close correspondence to elevated effective vegetation water content in the AMSR-E surfaces (Figure 4) and, to a lesser extent, soil moisture. The 2009  $\sigma_{of}$  mosaic, which is relatively seamless, exhibited low effective vegetation moisture content throughout the state apart from some coastal areas and again, the Carnarvon Gorge region. These latter cases can be explained by large-scale surface roughness because of topographic influences elevating the vegetation water content estimates [20]. This effect could potentially be removed if the minimum effective vegetation moisture content for each pixel within a time series was subtracted from the estimate. This would allow the remaining change to be interpreted solely as vegetation water content, although further research on this topic is required. Of note, is that JAXA also released the first 50 m mosaic of Australia for 2009.

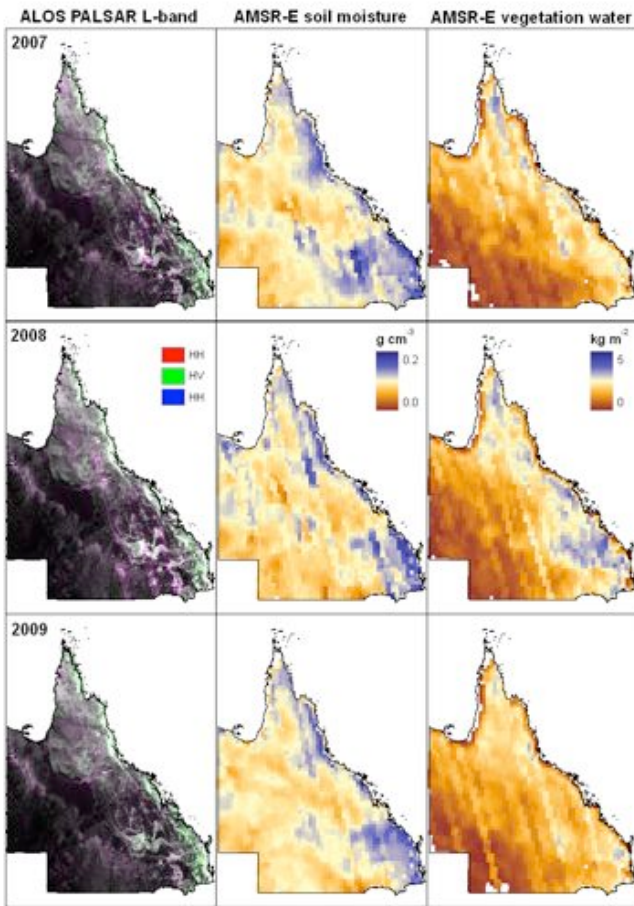


Figure 4. Annual mosaics of  $\sigma_{of}$  for Queensland for 2007, 2008 and 2009 generated based on the minimum average L-band HH. The corresponding AMSR-E soil moisture and effective vegetation moisture content for the times of PALSAR image acquisitions are also shown.

For all years, south-east Queensland and the coastal regions exhibit elevated soil moisture. The majority of these areas supports moderate to dense vegetation cover, including tropical and subtropical rainforests, which would bias the soil moisture estimates towards higher values [19].

An example of the impact of ground moisture conditions on a time series of the HH and HV polarised data is shown for a sample of pixels from RSP 374 (Figure 5). The magnitude of difference in  $\sigma_{of}$  between dates is greater for HH (up to 3 dB) than for HV (up to 2 dB) polarisation but the same bias is observed. Dates with similarly low effective vegetation water content have a 1:1 relationship and correspond to within  $\sim 1$  dB.

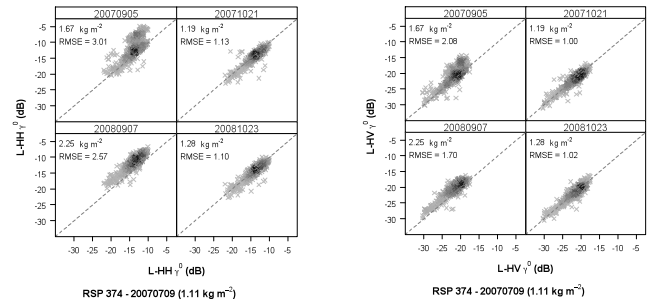


Figure 5. Consistency of L-HH (left) and L-HV (right) backscatter from 2007 to 2008 acquisition dates for RSP 374 when compared to the strip with minimum effective vegetation water content.

The L-HH  $\sigma_{of}$  bias for 5<sup>th</sup> September (Figure 5) is also illustrated spatially in Figure 6. Areas of woody vegetation and pastures exhibit higher  $\sigma_{of}$  compared to when observed on the 21<sup>st</sup> October, 2007. An interesting observation is the appearance of rain “bands” across the 5<sup>th</sup> September 2007 image, which highlight that ground water following rainfall strongly affects the backscatter at HH polarization.

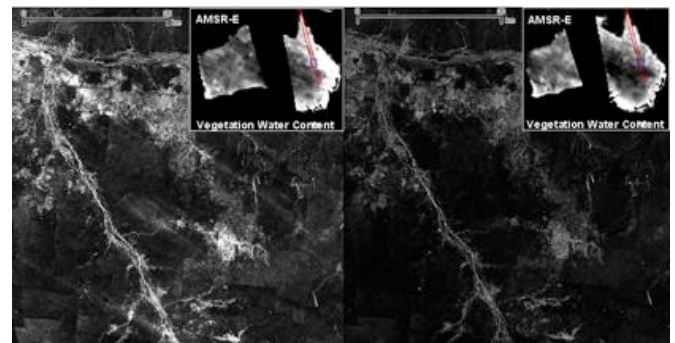


Figure 6. L-HH image for a “wet” (left) and a “dry” (right) acquisition date for RSP 374. AMSR-E effective vegetation water content data for the corresponding dates are shown (inset).

#### D. Regional mosaics of ALOS PALSAR and Landsat FPC

For Queensland, FPC is directly retrieved from Landsat sensor and ancillary (e.g., climate data; [9, 10]) data and provides a quantitative measure of foliage cover (of woody vegetation). By contrast, the L-band microwave interactions associated with the HH and HV data are primarily the result of double bounce scattering with the trunks and volume scattering from larger branches respectively. Hence, by combining these layers, information on different woody and foliar structures of vegetation is obtained. As illustration, an example of a composite Landsat FPC and ALOS PALSAR L-band HH and HV image is given in Figure 7, which shows areas of low woody vegetation (e.g., regrowth, scrub; red), higher biomass forest (pink to green) and cotton cultivation (different cycles; various colours in centre of image).

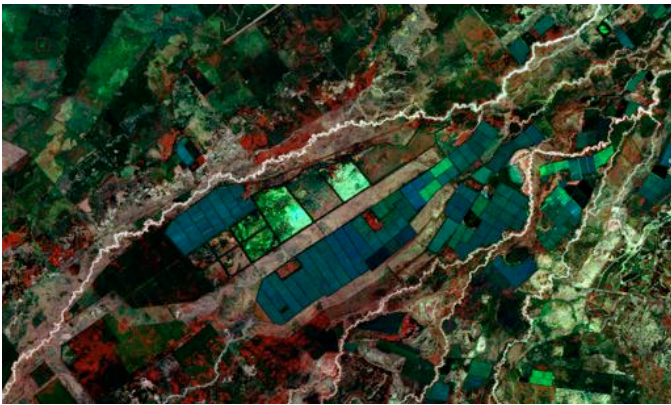


Figure 7. Composite of Landsat FPC and ALOS PALSAR L-band HH and HV, Queensland/NSW border.

Statewide Landsat FPC mosaics are generated annually and those for 2007 and 2008 were combined with the ALOS PALSAR HH and HV mosaics for the equivalent years. To some extent, the integrity of the mosaics (e.g., Figure 7) was compromised in some areas by the across track variability and between-image differences (including that associated with the Landsat FPC, although to a far lesser degree). However, unique information on vegetation and other surface structures is provided. The combination of these data therefore provides new regional datasets that can assist characterization and mapping of a range of forest structural types, including growth stage (particularly regeneration stage and standing dead or senescent timber). New information on the distribution and characteristics of wetlands (including mangroves) is also provided.

The 2009 Landsat FPC mosaic is in the process of being generated by QDERM and, when combined with the relatively seamless 2009 ALOS PALSAR HH and HV mosaic, is anticipated to provide the best available dataset for vegetation structural classification. It should be noted that Landsat FPC data are not produced for the Northern Territory and have only been recently generated for NSW.

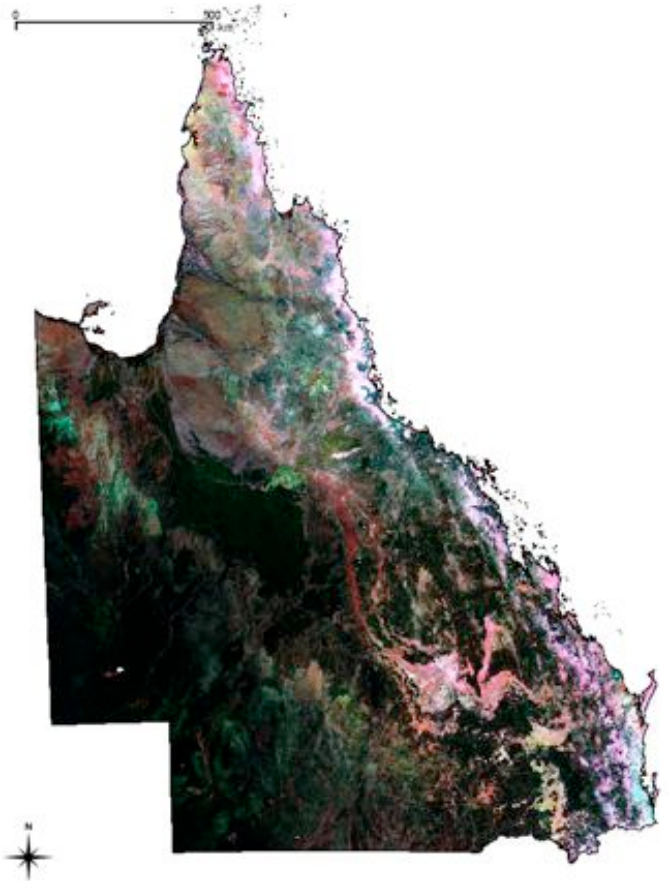


Figure 8. Landsat FPC, ALOS PALSAR HH and HV (in RGB) mosaic of Queensland, Australia, for 2007

## V. BIOMASS ESTIMATION

### A. Generation of a biomass library

To provide the opportunity to investigate the relationships between AGB and ALOS PALSAR data for the diverse range of vegetation communities occurring across Queensland, the collation of field data acquired over a similar time-frame as the PALSAR was operating (i.e., 2007 to 2009) and the generation of robust and consistent estimates of AGB through appropriate application of allometric equations was needed. For this purpose, field measurements of tree size and species type were collated from 19 studies conducted in Queensland, largely over the period 2005 to 2009 (Figure 9; [4]). For each plot, a polygon representing, as best as possible, dimensions and orientations, was generated. A total of 2781 plot-based measurements were included, although a number of plots (transects) were established to represent a particular forest or woodland community and hence some data were combined. When plot locations were overlain onto Landsat sensor and other remote sensing data (including aerial photographs), a number were also omitted from further analysis because of, for example, clearance events occurring in the period between measurement and ALOS data acquisition or low confidence in their location. This resulted in 1815 locations being used to establish relationships with the ALOS PALSAR data.

Following collation, the AGB was estimated for the range of tree species occurring using published allometric equations. Seven equations were selected, with these based on the relative behaviour of the functions across the size range, structural formations and wood densities. Both generic and genus-specific equations were utilised. Correction factors were applied to account for the AGB held within trees of varying conditions of health and both the live and dead AGB was estimated for all trees with a diameter at breast height (DBH) of  $\geq 5$  cm.

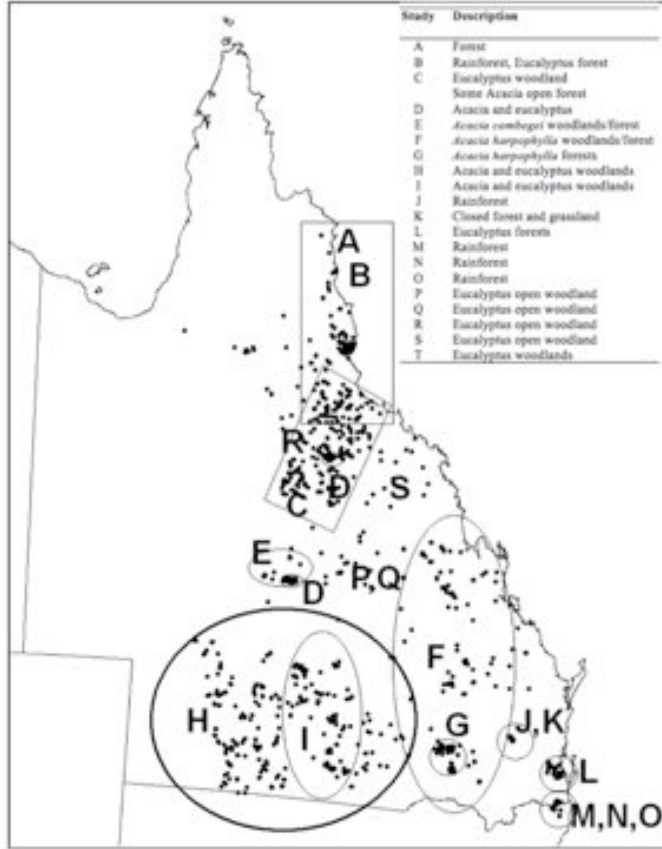


Figure 9. The location of sites in Queensland with available field-based measurements of tree size.

For the 1815 locations, L-band HH and HV data were extracted from all 2007 ALOS PALSAR strips, regardless of prevailing moisture conditions, and then converted to decibels (dB). For each location, RE pre-clearing codes were extracted and used to assign each location to a forest, woodland or open woodland structural formation and remnant or non-remnant status code. Relationships between AGB and both L-band HH and HV  $\sigma_f^0$  (with topographic and incidence angle correction) were then established for each structural formation. For all structural formations, a non-linear relationship between AGB and L-band  $\sigma_f^0$  was observed, as with many other studies, which was described using the backscatter model of [21] such that:

$$\sigma_f^0(\text{dB}) = a + e^{-(b\text{AGB}+c)} \quad (1)$$

where  $a$  is the saturation level in dB,  $b$  is the gradient of the curve at low biomass and  $c$  relates to the nominal backscatter from bare soil

### B. Relationships between AGB and L-band SAR data

Relationships based on L-band HH and HV data acquired under different moisture conditions and as a function of structural type are shown in Figure 10.

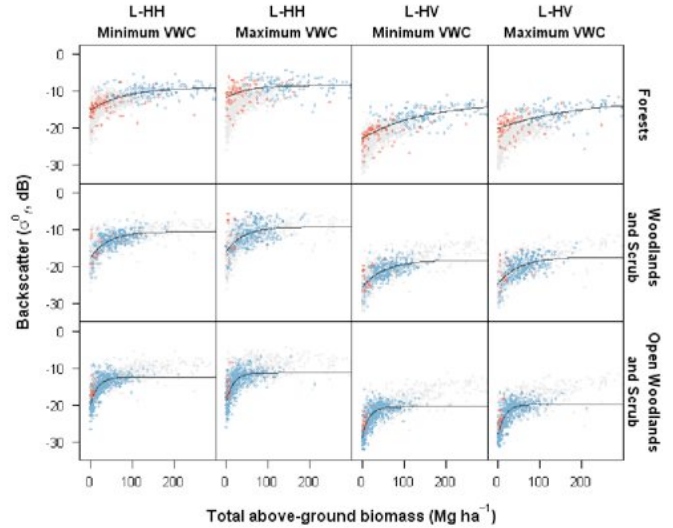


Figure 10. Relationships between AGB and L- band HH and HV  $\sigma_f^0$  for forests, woodlands and open woodlands (up to 300  $\text{Mg ha}^{-1}$ ), based on ALOS PALSAR data acquired during periods of relative minimum and maximum vegetation water content (VWC). Remnant and non-remnant forests are indicated in blue and red respectively. Remaining points in the dataset that were not used to generate the curve fits for forests, woodlands or open woodlands are shown in grey.

To establish differences in the relationship between structural formations, the point at which a change in  $\leq 0.01$  dB for a  $1 \text{ Mg ha}^{-1}$  of AGB was reached was identified. This point is referred to here as the ‘saturation level’ but it should be recognised that the approach and criteria used to define such a level can be subjective. The purpose of the exercise was therefore to simply establish relative differences in a defined ‘saturation level’ between structural formations and as a function of relative moisture conditions. When data acquired during relatively dry conditions were used, L-band HV  $\sigma_f^0$  for forests saturated (based on the criterion outlined above) at approximately  $270 \text{ Mg ha}^{-1}$ . For woodlands and open woodlands, saturation levels were comparatively lower at  $120$  and  $65 \text{ Mg ha}^{-1}$  respectively. At L-band HH, the saturation levels were similar. When compared to data acquired during wetter conditions, the L-band HV  $\sigma_f^0$  saturation level for forests remained the same, but at the lower end of the AGB range, which was associated with non-remnant forests,  $\sigma_f^0$  increased by 2-3 dB, which resulted in a reduction in the

dynamic range from 8.3 dB to 5.9 dB. Hence, the extent to which different magnitudes of AGB could be discriminated was reduced. For woodlands and open woodlands, a slight increase in the RMSE was observed (from 2.0 to 2.6 and 2.15 to 2.2 dB respectively) under wetter conditions.

At L-band HH, the AGB at which saturation occurred was reduced by over 100 Mg ha<sup>-1</sup> for forests (to ~ 100 Mg ha<sup>-1</sup>) and the dynamic range was reduced from 5.41 to 2.74 dB. The greatest increase in L-band HH  $\sigma_f^o$  saturation (> 4 dB) was observed within the non-remnant forests of lower AGB, with these primarily associated with those dominated by *A. harpophylla* (brigalow). The saturation level remained relatively similar for woodlands and open woodlands, primarily because the moisture differences between the driest and wettest dates were less.

### C. Regional mapping of AGB

Using a single relationship established for all remnant structural formations (forest, woodlands and open woodlands) and based on the mosaic generated using data acquired during periods of minimal effective vegetation moisture, a provisional map of the AGB for Queensland was generated (Figure 11). As with other studies, the mapping conveyed the confinement of the higher biomass forests to the eastern coast and the large expanse of lower biomass woodlands in the interior and north.

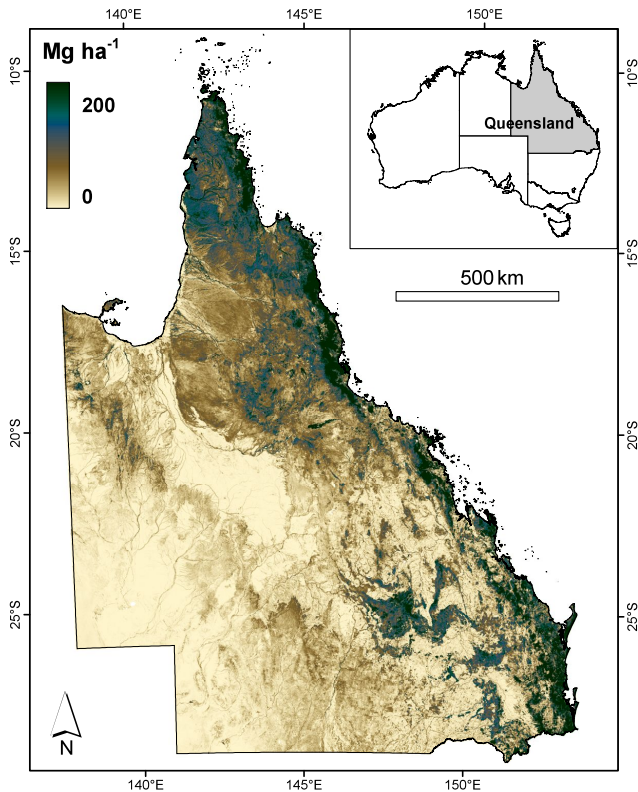


Figure 11. Map of AGB generated for Queensland using a relationship established between L-band HV  $\sigma_f^o$  and AGB.

### A. The Brigalow Belt Bioregion.

The discrimination and mapping of forest growth stage focused on the Brigalow Belt Bioregion of Queensland, where clearance and regeneration of woody vegetation has been extensive. The bioregion extends across the temperate, semi-arid tropical and subtropical regions of eastern Australia, occupies an area of approximately 36.5 million ha and includes 169 different Regional Ecosystems. 41.9 % of all ecosystems occurring prior to clearing are still considered to be remnant [11]. Brigalow is dominant, co-dominant or sub-dominant in 12 ecosystems and, within this area, the extent of remnant vegetation has been mapped through reference to historical aerial photography and reassessed through reference to up-to-date clearing histories generated using Landsat sensor time-series data [10]. Landsat FPC data have also been used to map the extent of regrowth across the bioregion by [22][23] using thresholds of 18 % and 9 % respectively, with the latter selected to capture more diffuse regrowth. [22] also mapped different stages of regrowth (based on age) through reference to time-series of Landsat sensor data.

### B. Available field data

For the study, the field datasets of [24] and [25] were used. [24] measured 82 stands associated with brigalow and *Casuarina* species in central Queensland, with 77 used in this analysis. At each site, 4 x 50 m transects were positioned from 25-75 m and 125-175 m along a 200 m transect (for an associated bird survey) although, in some cases, the transect length was reduced to < 50 m. Sampling was conducted during two survey periods; September 2005 to February 2006 and June to August 2006. [25] collected data from 70 sites where brigalow was dominant or co-dominant within the regenerating forest community. At each site, data were collected from up to four 50 x 4 m transects (at least 50 m apart) with the transect width depending upon the density of stems. Sampling was undertaken between September and November, 2007. Within both studies, stem size, density, canopy height and crown cover were recorded and AGB was estimated subsequently using species-specific allometric equations (e.g., [26]). The age of the forests sampled was estimated with reference to time-series of aerial photography and SPOT HRG imagery [24] and farmer interviews [25]. For this study, these two datasets were standardized and then combined. The majority of plots measured by [24] were located in the Tara Downs region within RE 11.4.3 whilst those of [25] were more widely distributed between the REs occurring in the BBB. However, because of the low number of remnant forest sampled by [25] in the other REs, the structural characteristics of these were not compared. The eight of the 12 BBB brigalow REs that included the field plots represented 93.8% of the pre-clearing extent of brigalow communities in the Brigalow Belt Bioregion.

### C. Structural variables

Differences in biophysical attributes were summarized as a function of age (Figure 12). A notable characteristic of

remnant forests was that they supported a greater basal area ( $> \sim 17 \text{ m}^2 \text{ ha}^{-1}$ ; based on quartiles) and AGB ( $> \sim 75 \text{ Mg ha}^{-1}$ ) and a lower density (typically  $< 3500 \text{ stems ha}^{-1}$ ) compared to younger forests. However, regrowth forests rapidly attained a canopy cover that was similar to remnant forests after  $\sim 20$ -30 years. Median canopy height (excluding emergents) was greatest (typically  $> 7 \text{ m}$ ) for remnant forests, with some overlap with the older regrowth forests ( $> \sim 40$  years).

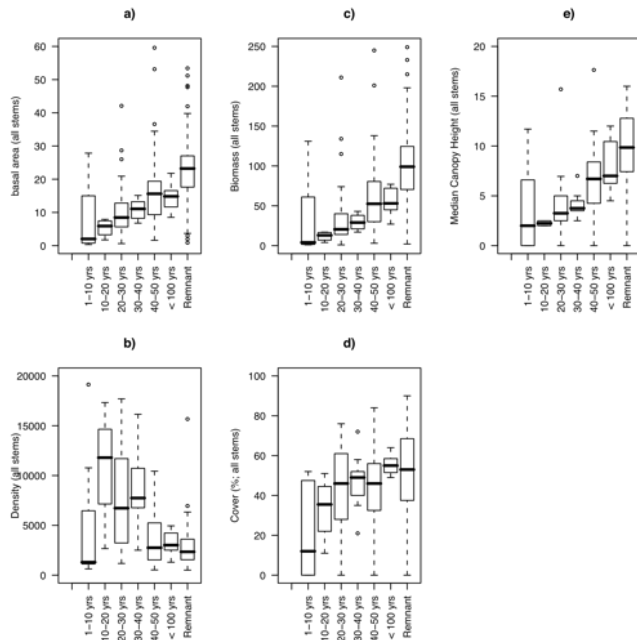


Figure 12. Variations in a) basal area, b) Above Ground Biomass (AGB), c) median canopy height, d) stem density and e) canopy cover as a function of age based on the combined dataset of Bowen (2009) and Dwyer (2010). The median is the line in the centre of the box, the two ends of the boxes represent the first and third quartiles, whilst the extremes represent the minimum and maximum of the datasets

#### D. Approach to mapping

The mapping of remnant, regrowth and cleared vegetation was confined to areas in the Brigalow Belt Bioregion, where brigalow communities were dominant, co-dominant or sub-dominant within the pre-clearing vegetation ([27][28]), and utilized both the Landsat FPC and ALOS PALSAR data. The high level of co-registration between these two datasets was particularly beneficial for this purpose.

The approach to mapping the *earliest stage of regrowth* was based on that outlined in [29]. This growth stage is associated with a high density of stems (often  $> 8000 \text{ ha}^{-1}$ ) collectively supporting a significant canopy cover, with few being of a size to evoke double bounce scattering at L-band (typically  $< 2 \text{ m}$  in height). Such areas were identified as supporting an L-band HH  $\sigma_f$  equivalent to non-forest (estimated at  $< -14 \text{ dB}$ ) and an FPC associated with woody vegetation. In this latter case, an FPC threshold of  $\geq 8\%$  was

applied to capture more scattered areas of early regrowth (i.e.,  $> 8 \%$ ), with this determined through reference to high-resolution (e.g., IKONOS) images (available through Google Earth) and aerial photography.

Whilst the Queensland Herbarium had previously determined the extent of *remnant forest* based on aerial photography and Landsat sensor data, an alternative approach to discrimination was developed, with this also based on a combination of Landsat FPC and ALOS PALSAR data. As indicated earlier, forests are defined as remnant where the dominant canopy contains species characteristic of the vegetation's undisturbed canopy and has  $> 70 \%$  of the height and  $> 50 \%$  of the cover relative to the height and cover of that stratum. This same principal was therefore applied to the mapping of remnant forest using ALOS L-band HH and HV and Landsat FPC data. First, the mapping was confined to the area associated with the pre-clearing extent of forests with brigalow as a component ([27]). Second, thresholds of L-band HH and HV and FPC were defined with reference to relationships observed with height, biomass and canopy cover respectively for selected RE's where field data had been collected for a range of growth stages.

Using FPC data alone, differentiation of remnant from all other regrowth stages was not possible because of similarities in canopy cover (Figure 12), although remnant forests typically supported a canopy cover at the higher end of the range. Remnant forests also exhibited comparatively higher values of L-band HV and HH  $\sigma_f$  compared to regrowth forests and a correspondence with AGB and median canopy height respectively was observed. On this basis, the extent of remnant forests was mapped using a combination of Landsat FPC and L-band HH and HV  $\sigma_f$ , with thresholds of  $< 30 \%$ ,  $-12 \text{ dB}$  and  $-17 \text{ dB}$  respectively. These thresholds were defined through reference to the observed extent of remnant forests in areas with field data but also the Queensland Herbarium mapping of remnant forest in these same areas. Whilst it is recognised that thresholds might vary as a function of RE and environmental conditions, these were considered appropriate at a regional level.

All remaining forest areas with an FPC  $> 12\%$  were associated with an *older growth stage*. This growth stage coverage a range of structures and further differentiation can potentially be achieved using relationships established with L-band SAR data or through reference to already derived products (e.g., AGB).

#### E. Regional maps of forest growth stage

The mapping of all growth stages was undertaken within eCognition by initially segmenting the Landsat FPC mosaic into objects up to a few pixels in size. Then, within the area associated with the pre-clearing extent of forests with brigalow as a component, the thresholds defined above were applied progressively to distinguish non-forest and forest (including diffuse regrowth), early regrowth, remnant forest and finally older regrowth. The resulting objects were then merged to generate the final map. The accuracy of the mapping was assessed independently through reference to 190

randomly generated locations for which time-series of Landsat sensor data, SPOT High Resolution Geometric (HRG) and historical aerial photography were available.

The map of growth stage for the BBB is presented in Figure 13 and highlights the fragmentation of the forests and their existence within a sea of agriculture. This study estimated that the extent of the 12 BBB pre-clearing ecosystems with brigalow as a component was over nine million ha. Within this area, 833,333 ha were mapped as the early stage of regrowth, with this associated with a high density of stems of small size. Remnant forests and older regrowth forests were estimated to cover an area of 625,529 ha and 604,110 ha respectively. The remaining area of almost seven million ha had been cleared without any regrowth detected.

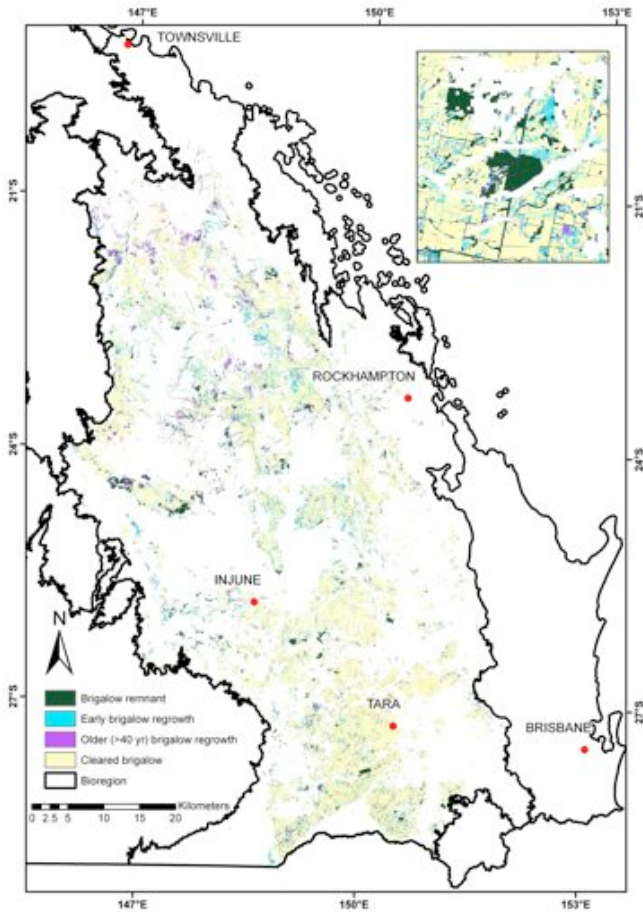


Figure 13. The extent of brigalow remnant and regrowth stages mapped using a combination of ALOS PALSAR L-band data and Landsat FPC.

#### F. Accuracy of classification

The accuracy of the growth stage classification was quantified through reference to 190 sites for which aerial photography and other higher resolution (e.g., SPOT HRG) data were available. Of these, 121 (86.4 %) were correctly classified as regrowth (early and older regrowth combined), with 14 and 5 sites misclassified as cleared land and remnant

forest respectively (Table Ia). In the classification of remnant forest, 45 (90 %) sites were correctly assigned, with most confusion being with regrowth forest. When the regrowth classes were considered separately (Table Ib), most confusion was between remnant and early regrowth forests, which was attributed in part to land cover change. In the classification of early regrowth, which relies on the integration of L-band HH and Landsat-derived FPC, 59 (75.6 %) of sites were correctly classified with confusion occurring with both cleared and older regrowth but less so remnant vegetation. The accuracy in the classification of older regrowth was 54.8 %, with this largely attributed to confusion with early regrowth. The structural characteristics of forests transitioning from early to late regrowth are difficult to describe, even from field measurements, and so this confusion is not unexpected. However, future work needs to better establish (for the different REs), the structural characteristics of forests in the transitions between stages, and understand how these are manifested within radar and optical remote sensing data.

Table I. Accuracies in the classification of a) regrowth, remnant and non-forest (cleared) and b) early regrowth, older regrowth, remnant and non-forest (cleared).

a) Classification		
Assessment	Regrowth	Remnant
Cleared	14	0
Regrowth	121	5
Remnant	5	45
	86.4%	90.0%

b) Classification			
Assessment	Early Regrowth	Older Regrowth	Remnant
Cleared	9	5	0
Early Regrowth	59	20	4
Older Regrowth	8	34	1
Remnant	2	3	45
	75.6%	54.8%	90.0%

#### G. Clearing mechanisms

Throughout Queensland, a number of methods are used for clearing vegetation including chaining and stem injection. The potential of SAR data for establishing the methods of clearing was highlighted by [6], with this based on observations using NASA Jet Propulsion Laboratory (JPL) AIRSAR data. However, similar patterns were observed within the ALOS PALSAR data. For example, rows of trees pulled over by dragging a chain between two bulldozers exhibited a high L-band HH response [30]. Furthermore, areas of dead standing timber were identified as these exhibited a high L-band HH and low FPC compared to woody vegetation with foliage cover. However, reference to ground observations undertaken within

the Injune study area in April, 2009, suggested some confusion with bare ground, with this attributed only in part to woody debris on the surface. Other contributory factors included surface roughness but also differences in soil and vegetation moisture content between cleared areas.

## VII. DETECTION OF CHANGE

### A. Time-series comparisons of SAR data

The generation of regional ALOS PALSAR mosaics for 2007, 2008 and 2009 highlighted the impacts of ground moisture on the L-band HH and, to a lesser extent, HV  $\sigma_f$  and the increasing saturation of  $\sigma_f$  with AGB. Comparison of ALOS PALSAR and also JERS-1 SAR data (Figure 14) confirmed that changes in the woody components of vegetation could be detected over decadal periods. However, over shorter periods (e.g., the year operation period of the ALOS PALSAR), distinguishing changes attributed to growth or loss of woody vegetation rather than ground moisture differences was more difficult. Even within the same year, differences of up to  $\sim 4$  dB and  $\sim 2$  dB were observed within L-band HH and HV data respectively.

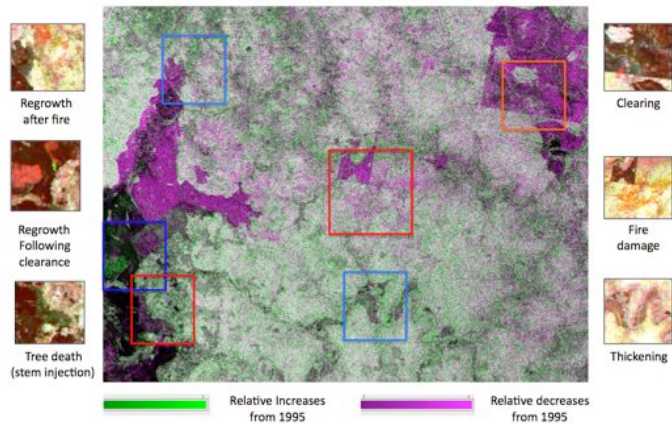


Figure 14. Relative increases and decreases in L-band HH backscatter observed through time-series comparison of ALOS PALSAR and JERS-1 SAR data for the Injune Landscape Collaborative Study Area. Inset images are composites of Landsat FPC and ALOS PALSAR HH and HV data in RGB.

A further limitation was that whilst areas cleared or vegetation could be readily distinguished, the more subtle changes associated with forest regeneration, thickening and degradation of woody vegetation were more difficult to identify. Even if areas of change are identified, validating the nature and magnitude of the change has provided problematic over such large areas. For this reason, regional products of AGB change have not yet been generated, even though mosaics of ALOS PALSAR data were produced for Queensland for 2007, 2008 and 2009. Instead, focus has been on the analysis of time-series of airborne LiDAR and multi-/hyperspectral datasets acquired across a range of vegetation structural types in Queensland. These fine spatial resolution change datasets will serve to better understand and validate how change is manifested within and can be best-detected using multi-

temporal ALOS PALSAR data. Research is also focusing on better establishing the influence of soil and vegetation water content on ALOS PALSAR backscatter data.

### B. Provision of validation datasets

For over 20 sites in Queensland ranging from mulga (*Acacia aneura*) open woodlands to closed tropical rainforest, airborne LiDAR data were acquired in 2004/5 and again in 2008. These datasets are currently being analysed by QDERM to identify and quantify change at the individual tree and stand level. Furthermore, over the Injune Landscape Collaborative Project (ILCP) study area in central southeast Queensland, discrete return LiDAR and hyperspectral Compact Airborne Spectrographic Imagery (CASI) and 1:4000 aerial photography were acquired over 150 500 x 150 m sampling units in 2000 [31]. In 2009, a second airborne campaign was undertaken to establish whether changes in the species composition, structure and biomass of forests occurring as a consequence of both natural and anthropogenic (including climate) change could be detected and quantified. An example of such changes is given in Figure 15 which highlights the loss of individual trees within an ‘intact’ woodland.

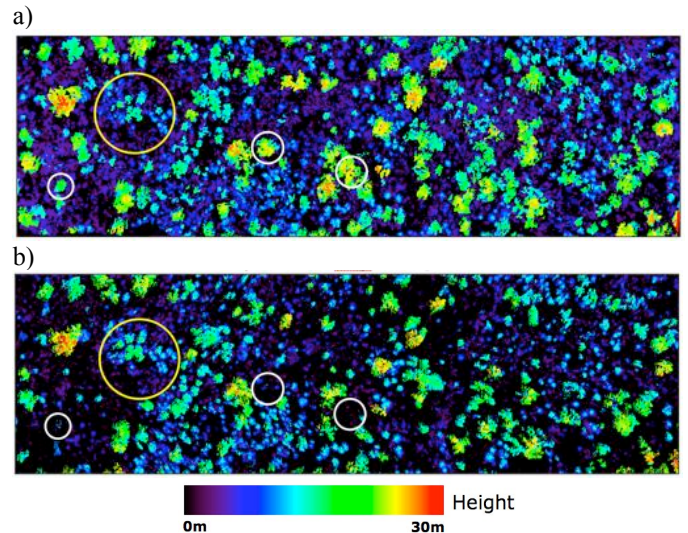


Figure 15. a) Optech ALTM1020 and b) Riegl LMS-Q560 data acquired over one (of 150) 500 m x 150 m area within the Injune Landscape Collaborative Project in 2000 and 2009 respectively.

## VIII. DISCUSSION

### A. Biophysical retrieval and classification: impacts of ground moisture

The use of ALOS PALSAR data acquired during relatively dry conditions is a pre-requisite to the retrieval of and detection of change in biophysical attributes and also classification of land covers (e.g., vegetation structural formations). To identify scenes acquired under relatively dry conditions, reference can be made to a number of datasets including interpolated or actual (e.g., Tropical Rainfall

Measuring Mission (TRMM)) rainfall data and soil/vegetation moisture surfaces from AMSR-E or new sensors (e.g., the European Space Agency's (ESA) Soil Moisture and Ocean Salinity (SMOS) mission). AMSR-E and SILO data are currently available free of charge and are a useful tool for selection of appropriate ALOS PALSAR image dates. Although AMSR-E products, as with PALSAR, are derived from microwave remote sensing, their high temporal resolution coverage permits wall-to-wall assessment of relative changes in soil moisture and vegetation water content over time. The use of relative rather than absolute moisture conditions is considered appropriate when selecting scenes, particularly given the uncertainty in retrieval of soil and vegetation moisture from currently operating sensors (which results partly from their relatively coarse spatial resolution). However, further research is needed to better establish the impact of soil and vegetation moisture on SAR backscatter as this would lead to better retrieval of AGB and potentially ground moisture itself. In the ideal situation, the image archives of ALOS PALSAR data should be linked directly with data relating to ground moisture conditions during the time of acquisition such that the most appropriate datasets can be utilised. The lack of provision of such information in the past has most likely led to the high variability in relationships and saturation levels reported previously between AGB and other structural attributes and SAR data.

A number of studies have established that retrieval of AGB may be enhanced by using multi-temporal data and filtering algorithms (e.g., [32]) as speckle noise is reduced. A potential limitation of this approach is that by using data from several years, as would be the case of ALOS PALSAR, the opportunities for detecting changes in AGB would be reduced unless, for example, comparisons on a five year interval were acceptable. This is not unreasonable in the case of detecting changes in AGB, given the generally slow rates of accumulation within woody vegetation and losses through degradation. Areas of more rapid AGB loss through clearing could be identified through reference to existing land cover change datasets (e.g., the Statewide Land Cover and Trees Study (SLATS; [10], with associated estimates of AGB derived from ALOS PALSAR data being potentially more robust because of the use of multi-temporal datasets.

#### B. Impacts of vegetation structure on retrieval of AGB

In retrieving AGB (ideally from relatively dry scenes), consideration still needs to be given to differences in structure between vegetation types. In the mapping of AGB, a single relationship based on all forest types has been applied. However, separate relationships could equally be used for forests, woodlands and open woodlands although reliable *a priori* mapping of these structural formations is essential. Much of the differences in the relationships observed with AGB between these formations was attributable to variations in density and size class distribution and so an algorithm that takes account of these structural attributes is desirable, with one approach being that of non-linear estimation [33]. Differences in the rate of change in backscatter with AGB

may also be a function of the state of growth, with most regrowth (non-remnant) stands being the result of human intervention and consequently exhibiting relative homogeneity in terms of tree size. Consideration also needs to be given to the size class distribution of woody components. In the Brigalow Belt Bioregion, a characteristic of the extensive tracts of early regrowth dominated by brigalow is that they support a high density of stems (typically > 8000) with most being of relatively small size. Observations using polarimetric C, L and P-band SAR data [29] conveyed that whilst these forests exhibited a high C-band backscatter from the foliage and small branches, the stems were of insufficient size to evoke a response at both L- and P-band. The study therefore highlighted that L-band SAR is not sensitive to all of the AGB contained within woody vegetation and underestimates at the stand level may occur, particularly for regrowth, understorey and heathland vegetation.

#### C. Biomass estimation

Whilst the mapping provides a reasonable representation of the distribution of AGB, there are several limitations. In particular:

a) Landsat-derived FPC within empirical relationships, particularly as L-band HH and HV are sensitive primarily to the trunk/stem and branch biomass respectively and FPC is indicative of the vertical distribution of foliage [9][10].

b) The saturation of the relationship between AGB and L-band HV  $\sigma^0$  leads to greater errors as AGB increases and lower accuracies in retrieval for forests supporting higher levels of AGB.

c) Differences in the relationships observed between structural formations and as a function of regeneration stage (i.e., remnant and non-remnant) are not considered.

d) Areas associated with enhanced L-band backscatter because of underlying geology or the presence of urban areas and infrastructure are not compensated for.

e) Local enhancement in L-band  $\sigma^0_f$  is still evident in areas of localised rainfall and increased ground moisture (e.g., near Carnarvon Gorge).

For this reason, a number of options for providing more robust estimates of AGB require development. These should ideally focus on generating a baseline map of AGB using data acquired over the shortest time frame (i.e., within a year), thereby providing better opportunities for detecting changes in AGB that occur in response to natural or anthropogenic change (including those associated with climatic fluctuation)

#### D. Approaches to refining biomass estimates

Proposed options for improving estimates of AGB include the use of:

a) Landsat-derived FPC within empirical relationships, particularly as L-band HH and HV are sensitive primarily to the trunk/stem and branch biomass respectively and FPC is indicative of the vertical distribution of foliage.

b) Non-linear estimation algorithms [33] that use modeling to establish relationships between backscatter and a limited number of unknowns having the largest effect on overall backscatter.

In some areas, the enhancement of L-band backscatter was evident because of geology and infrastructure. For this reason, any attempt at regional retrieval of AGB needs to take into account the mapped extent of urban areas, other surfaces (e.g., exposed rocks) and even metal structures (e.g., fences). The use of PALSAR polarimetric coherence may assist here as some geological formations and urban environments exhibit high coherence compared to vegetation. A further option is to include climate surfaces or models of predicted AGB to constrain the estimates generated using the methods outlined above. Consideration should also be given to vegetation types that are known to exhibit different responses at L-band. These include flooded forest (e.g., *Melaleuca*-dominated stands), which are often associated with an enhanced backscatter particularly at L-band, and high biomass mangroves with prop root systems which typically support an L-band HH and HV return similar to non-forest that decreases with increasing biomass [34]. Existing floristic mapping in Queensland may be used to inform on the extent of these vegetation types ([35]).

#### E. Growth stage classification

Using the combination of Landsat FPC and ALOS PALSAR data, three classes of regrowth (including remnant) with brigalow as a component were classified, with discrimination based on defined thresholds. To discriminate early regrowth forests from non-forest, an FPC threshold of 8 % was necessary to capture areas of woody regrowth that were more scattered and hence supported a lower canopy cover. This threshold was below the 12 % used commonly to distinguish forest from non-forest (which approximates to 20 % canopy cover) and the 9 % used by [23] but was considered most appropriate for mapping areas of early and less contiguous regrowth identified within available fine resolution datasets. Whilst woody vegetation associated with this lower FPC is not strictly defined as forest, areas identified have the potential to become forest in future years and hence their inclusion is justified.

Within the mapped area, the differentiation of growth stage required the combination of ALOS L-band HH and HV and also Landsat FPC; when these channels were used alone, differentiation could not be achieved. The approach to classifying the early regrowth stage was supported by the study of [29] using airborne SAR (AIRSAR) and SAR simulation models. This study demonstrated that stems need to be  $< \sim 2.5 - 3$  m in height for double bounce scattering to occur, with this being the primarily mechanism contributing to the L-band HH return [36]. Hence, data acquired at this polarisation were

pivotal to the classification of early regrowth. A particular advantage of this approach was that the regrowth class was defined with reference to a quantifiable biophysical attribute (i.e., FPC) and a recognisable point of transition between specular and double bounce scattering at L-band.

The discrimination of remnant forest from all regrowth stages used the same principle as field-based definitions, which are based on a relative comparison of height and cover. Higher values of L-band HH and HV were generally associated with remnant forests of greater median canopy height and AGB and remnant forests typically supported a canopy cover (and hence FPC) that was at the upper end of the observed range. Remnant forests were therefore defined as those that collectively exhibited higher values of L-band HH and HV and FPC compared to younger growth stages. Over 90 % of sites known to be remnant forest were correctly classified and the mapped extent corresponded closely to the areas defined as remnant through the RE mapping.

The definition of the older growth stage is dependent upon reliable differentiation of the early regrowth stage and remnant forest. However, for discrimination of both, the thresholds were defined using data acquired unevenly and for only eight of the 12 BBB brigalow REs in Queensland. Hence, a more logical approach, and one that is currently being investigated is to use variable thresholds for each RE, thereby accounting for local differences in these data as a function of, canopy height, cover, AGB and other structural attributes.

The estimates of the extent of forest growth stages reported in this study are indicative and based largely on single thresholds applied to Landsat FPC and PALSAR L-band HH and HV mosaics; these may be adjusted in later revisions of the mapping. To increase the accuracy of this mapping, further refinements are being implemented including a) the use of thresholds specifically derived for each RE and b) integration of additional field data to better define the transitions from non-forest through to regrowth and remnant forests and the associated manifestation within remote sensing data.

## IX. CONCLUSIONS

### A. Pre-processing and impacts of ground moisture

- The use of Landsat sensor panchromatic data in the geocoding procedure allows reliable co-registration of ALOS PALSAR strip data with existing thematic datasets.
- Through reference to AMSR-E soil and effective vegetation water content surfaces, the adverse influence of ground moisture conditions on ALOS PALSAR backscatter and relationships formed with AGB has been highlighted.
- Regional mosaics of PALSAR data were generated from strips associated with relatively minimal L-band HH backscatter, with these corresponding closely with periods of minimal ground moisture. The use of these data avoided the need for brightness correction algorithms, within and between strips.
- Daily AMSR-E soil moisture and effective vegetation water content images, available for the entire life of

ALOS PALSAR, are therefore advocated as a standard ancillary data product for selection and interpretation of PALSAR imagery over large areas and over time.

#### B. AGB estimation

- A statewide map of AGB has been generated for Queensland using data acquired during periods of relatively dry moisture conditions and a single relationship established between L-band HV  $\sigma_f^0$  and AGB. However, better mapping would most likely be achieved using relationships specific to different structural formations (e.g., forests, woodlands and open woodlands).
- Whilst the map provides a broad indication of the distribution of AGB in Queensland, saturation of the L-band HV above certain levels of AGB (which vary as a function of structural formation) is evident and discrepancies resulting from, for example, geology, infrastructure and unique signatures associated with some vegetation types (e.g., early regrowth, mangroves and flooded forest).
- The mapping could be refined also by including Landsat-derived FPC and ICESat GLAS-derived estimates of height into the retrieval algorithm. The use of multi-temporal data is advocated as long as the capacity for detecting changes in AGB is not compromised.
- Queensland is in a unique position to advance the mapping of AGB using algorithms that integrate ALOS PALSAR data because of the availability of interannual mosaic data and Landsat-derived FPC. The approaches developed can also be applied to other states in Australia if algorithms are adopted and appropriate datasets obtained.

#### C. Growth stage mapping

- By integrating Landsat-derived FPC and ALOS PALSAR L-band HH and HV data, maps of three growth stages (early regrowth, older regrowth and remnant forest) have

been generated for the Brigalow Belt Bioregion of central southeast Queensland.

- The first stage is uniquely defined by this combination of data and is based on a physical principle of L-band microwave interaction with the woody components of vegetation and a retrieved biophysical attribute (i.e., FPC). Whilst studies have quantified the extent of regrowth brigalow communities, the extent of the early regrowth stage was not previously known
- Remnant forests are identified as these exhibit comparatively greater values of ALOS PALSAR L-band HH and HV and Landsat FPC compared to non-remnant (including regenerating) forests.
- Most regrowth is attributed to the recovery of forests following the extensive clearing of vegetation in mid 1990s and early 2000s. Through effective management, these previously forested areas provide the best opportunity to restore the carbon and biodiversity lost through clearing. As such, the maps generated from this research can be used to identify and recommend areas most suitable for restoration of brigalow ecosystems.

#### D. Detection of change

- Annual (2007, 2008 and 2009) mosaics of ALOS PALSAR data have been generated for Queensland, Australia.
- Whilst these mosaics can be used to generate maps of AGB change, the uncertainties associated with ground moisture effects reduce reliability in detecting losses or gains in AGB (apart from through clearance events) and transitions between growth stages
- Confidence in the use of these data for detecting change is likely to increase following generation of tree to stand level change maps for selected sites through time-series comparison of airborne LiDAR datasets.

#### ACKNOWLEDGEMENTS AND IMAGE COPYRIGHTS

The work has been undertaken in conjunction with the Queensland Department of Natural Resources and Water (QDNRW) and the Queensland Herbarium and has been undertaken within the framework of the JAXA Kyoto & Carbon Initiative. ALOS PALSAR data have been provided by JAXA EORC." All illustrations are copyright of the ALOS K&C © JAXA/METI, QDNRW and Queensland Herbarium EPA.

#### REFERENCES

- [1] M.E. Bowen, C.A. McAlpine, A.P.N. House and G.C. Smith. Regrowth forests on abandoned agricultural land: A review of their habitat values for recovering forest fauna. *Biological Conservation*, vol.140, 273-296, 2007.
- [2] M.E. Bowen, C.A. McAlpine, L. Seabrook, A.P.N. House and G.C. Smith, "The age and amount of regrowth forest in fragmented brigalow landscapes are both important for woodland dependent birds". *Biological Conservation*, vol. 142, 3051-3059, 2009.
- [3] A. Rosenqvist, M. Shimada, N. Ito and M. Watanabe, "ALOS PALSAR: A pathfinder mission for global-scale monitoring of the environment," *IEEE Trans. Geosci. Remote Sens.*, vol. 45, no. 11, pp. 3307-3316, 2007.
- [4] R. Lucas, J. Armston, R. Fairfax, R. Fensham, A. Accad, J. Carreiras, J. Kelley, P. Bunting, D. Clewley, S. Bray, D. Metcalfe, J. Dwyer, M. Bowen, T. Eyre, M. Laidlaw and M. Shimada. An evaluation of the ALOS PALSAR L-band backscatter – above ground biomass relationship, Queensland, Australia: Impacts of surface moisture condition and vegetation structure. *IEEE Journal of Selected Topics in Applied Earth Observations and Remote Sensing (JSTARS)*, vol. 3, no. 4, pp. 576 – 593, 2010.
- [5] V.J. Neldner, B.A. Wilson, E.J. Thompson and H.A. Dillewaard, "Methodology for Survey and Mapping of Regional Ecosystems and Vegetation Communities in Queensland, Version 3.1," Queensland Herbarium Environmental Protection Agency, Brisbane, 2005.

- [6] R.M. Lucas, A. Accad, L. Randall, P. Bunting, and J. Armston, "Assessing human impacts on Australian forests through integration of airborne/spaceborne remote sensing data," In: *Patterns and Processes in Forest Landscapes: Multiple uses and sustainable management*, pp. 213-240, Ed. R. Laforzezza, J. Chen, G. Sanesi and T.R. Crow, Springer, 2008.
- [7] U. Wegmüller, C. Werner and T. Strozzi (1998). SAR interferometric and differential interferometric processing. *Proceedings of IGARSS'98*, 6-10 July, Seattle, pp. 1106-1108.
- [8] U. Wegmüller (1999). Automated terrain corrected SAR geocoding. *Proceedings of IGARSS'99*, 28 June – 2 July, Hamburg, pp. 1712-1714.
- [9] J.A. Armston, R.J. Denham, T. Danaher, P.F. Scarth and T.N. Moffiet, "Prediction and validation of foliage projective cover from Landsat-5 TM and Landsat-7 ETM+ imagery," *Journal of Applied Remote Sensing*, vol. 3, pp. 033540, 2009.
- [10] T. Danaher, P. Scarth, J. Armston, L. Collet, J. Kitchen and S. Gillingham, "Remote sensing of tree-grass systems: The Eastern Australian Woodlands" in: *Ecosystem Function in Savannas: Measurement and Modelling at Landscape to Global Scales*, Eds. M.J. Hill and N.P. Hanan, Taylor and Francis (in press).
- [11] A. Accad, V.J. Neldner, B.A. Wilson and R.E. Niehus, "Remnant vegetation in Queensland. Analysis of remnant vegetation 1997-1999-2000-2003-2005, including regional ecosystem information," Queensland Herbarium, Qld Environmental Protection Agency, 2008.
- [12] T. Castell, A. Beaudoin and N. Stach, "Sensitivity of space-borne SAR data to forest parameters over sloping terrain. Theory and experiment." *International Journal of Remote Sensing*, vol. 22, no. 12, pp. 231-2376.
- [13] M. Santoro, J.E.S. Fransson, L.E.B. Eriksson, M. Magnusson, L.M.H. Urlander and H. Olsson, "Signatures of ALOS PALSAR L-band backscatter in Swedish Forest," *IEEE Trans. Geosci. Remote Sens.*, vol. 47, no. 12, pp. 4001-4019, 2009.
- [14] C.J. Thiel, C. Thiel and C.C. Schmillius, "Operational large-area forest monitoring in Siberia using ALOS PALSAR summer intensities and winter coherence", *IEEE Trans. Geosci. Remote Sens.*, vol. 47, no. 12, pp. 3993-4000, 2009.
- [15] E.G. Njoku, T.J. Jackson, V. Lakshmi, T.K. Chan and S.V. Nghiem, "Soil moisture retrieval from AMSR-E," *IEEE Trans. Geosci. Remote Sens.*, vol. 41, no. 2, pp. 215-229, 2003.
- [16] E.G. Njoku, updated daily, "AMSR-E/Aqua L2B Surface Soil Moisture, Ancillary Params, & QC EASE-Grids V002, 2007 AMSR-E data," Boulder, Colorado USA: National Snow and Ice Data Center. Digital media, 2004.
- [17] L.J. Renzullo, D.J. Barrett, A.S. Marks, M.J. Hill, Guerschman, J.P., Mu, Q. and S. Running, "Multi-sensor model-data fusion for estimation of hydrologic and energy flux parameters," *Remote Sensing of Environment*, vol. 112, pp. 1306-1319, 2008.
- [18] S. Jeffrey, J.O. Carter, K.B. Moodie and A.R. Beswick, "Using spatial interpolation to construct a comprehensive archive of Australian climate data," *Environmental Modelling & Software*, vol. 16, pp. 309-3, 2001.
- [19] R. Bindlish, T.J. Jackson, A.J. Gasiewski, M. Klein and E.G. Njoku, "Soil moisture mapping and AMSR-E validation using the PSR in SMEX02. Remote Sensing of Environment", vol. 103, pp. 127-139, 2006.
- [20] E.G. Njoku and S.K. Chan, "Vegetation and surface roughness effects on AMSR-E land observations", *Remote Sensing of Environment*, vol. 2, pp. 190-199, 2006.
- [21] A. Luckman, J. Baker, M. Honzak, and R. Lucas, R, "Tropical forest biomass density estimation using JERS-1 SAR: Seasonal variation, confidence limits, and application to image mosaics". *Remote Sensing of Environment*, vol. 63, pp. 126-139, 1998.
- [22] D.W. Butler, "Planning iterative investment for landscape restoration: Choice of biodiversity indicator makes a difference." *Biological Conservation*, vol. 142, no. 10, pp. 2202-2216, 2009
- [23] Accad, A. unpublished 2009.
- [24] M.E. Bowen, "Quantifying the ecological values of brigalow regrowth for woodland birds: a hierarchical landscape approach". PhD thesis, School of Geography, Planning and Environmental Management, The University of Queensland, Brisbane, 2009.
- [25] J.M. Dwyer, "Tree growth and mortality and implications for restoration and carbon sequestration in Australian subtropical semi-arid forests and woodlands." PhD Thesis, The University of Queensland, Australia, 2010.
- [26] J.C. Scanlan, "Woody overstorey and herbaceous understorey biomass in *Acacia harpophylla* (brigalow) woodlands," *Australian Journal of Ecology*, vol. 16, pp. 521-529, 1991.
- [27] Queensland Herbarium, "Survey and Mapping of Pre-clearing Vegetation Communities and Regional Ecosystems of Queensland", Version 6.0b, November 2009, Department of Environment and Resource Management: Brisbane.
- [28] Queensland Herbarium, "Survey and Mapping of 2006b Vegetation Communities and Regional Ecosystems of Queensland", Version 6.0b, November 2009, Department of Environment and Resource Management: Brisbane, 2009.
- [29] R.M. Lucas, N. Cronin, M. Moghaddam, A. Lee, J.A. Armston, P. Bunting and C. Witte, "Integration of radar and Landsat-derived foliage projected cover for woody regrowth mapping, Queensland, Australia," *Remote Sensing of Environment*, vol. 100, pp. 388-406, 2006.
- [30] De Grandi, F., Lucas, R.M. and J. Kropacek, "Analysis by wavelet frames of spatial statistics in SAR data for characterizing structural properties of forests". *IEEE Trans. Geosci. Remote Sens.*, vol. 7, no. 2, 9-507, 2009.
- [31] P.K. Tickle, A. Lee, R.M. Lucas, J. Austin and C. Witte, "Quantifying Australian forest and woodland structure and biomass using large scale photography and small footprint Lidar," *Forest Ecology and Management*, vol. 223, pp. 379-394, 2006.
- [32] G.F. De Grandi, M. Leysen, J.S. Lee and D. Schuler, "Reflectivity estimation using multiple SAR scenes of the same target: techniques and applications", *Proceedings, IGARSS 1997 Remote Sensing – A Scientific Vision for Sustainable Development*, vol. 2, 1047-1050, 1997.
- [33] M. Moghaddam and S. Saatchi, "Monitoring tree moisture using an estimation algorithm applied to SAR data from Boreas." *IEEE Trans. Geosci. Remote Sensing*, vol. 37, pp. 901-916, 1999.
- [34] R.M. Lucas, A.L. Mitchell, A. Rosenqvist, C. Proisy, A. Melius and C. Ticehurst, "The potential of L-band SAR for quantifying mangrove characteristics and change: case studies from the tropics," *Aquatic Cons. Marine and Freshwater Ecosystems*, vol. 17, pp. 245-264, 2007
- [35] R.J. Fensham and G.P. Guymer, "Carbon accumulation through ecosystem recovery". *Environmental Science and Policy*, vol. 12, pp. 367-372, 2009.
- [36] R.M. Lucas, M. Moghaddam and N. Cronin, "Microwave scattering from mixed species woodlands, central Queensland, Australia." *IEEE Trans. Geosci. Remote Sensing*, vol. 42, pp. 2142-2159, 2004



**Richard Lucas.** Received the B.Sc. degree in biology and geography (First Class) and the Ph.D. degree in the remote sensing of snow and vegetation using AVHRR and Landsat sensor data from the University of Bristol, Bristol, UK, in 1986 and 1989 respectively. He is currently Professor at Aberystwyth University in Wales, UK, where he is involved primarily in the integration of single data and time-series radar, optical (hyperspectral) and LiDAR data for retrieving the biomass, structure and species/community composition of ecosystems ranging from subtropical woodlands to tropical forests and mangroves. His research has and continues to focus on the carbon dynamics of these systems and their response to natural and human-induced change. He has authored or co-authored over 100 journal articles, book chapters and conference papers